

## Thin layer thickness measurements by zero group velocity Lamb mode resonances

Maximin Cès, Dominique Clorennec, Daniel Royer, and Claire Prada

Citation: *Rev. Sci. Instrum.* **82**, 114902 (2011); doi: 10.1063/1.3660182

View online: <http://dx.doi.org/10.1063/1.3660182>

View Table of Contents: <http://rsi.aip.org/resource/1/RSINAK/v82/i11>

Published by the [American Institute of Physics](http://www.aip.org).

---

### Related Articles

Use of vehicle magnetic signatures for position estimation  
*Appl. Phys. Lett.* **99**, 134101 (2011)

High speed two-dimensional optical beam position detector  
*Rev. Sci. Instrum.* **82**, 073705 (2011)

Thermally exfoliated graphene based counter electrode for low cost dye sensitized solar cells  
*J. Appl. Phys.* **109**, 124308 (2011)

Influence of intensity loss in the cavity of a folded Fabry-Perot interferometer on interferometric signals  
*Rev. Sci. Instrum.* **82**, 063103 (2011)

Evaluation of an electrostatic dust removal system with potential application in next-step fusion devices  
*Rev. Sci. Instrum.* **82**, 053502 (2011)

---

### Additional information on *Rev. Sci. Instrum.*

Journal Homepage: <http://rsi.aip.org>

Journal Information: [http://rsi.aip.org/about/about\\_the\\_journal](http://rsi.aip.org/about/about_the_journal)

Top downloads: [http://rsi.aip.org/features/most\\_downloaded](http://rsi.aip.org/features/most_downloaded)

Information for Authors: <http://rsi.aip.org/authors>

### ADVERTISEMENT

**AIP**Advances

*Submit Now*

Explore AIP's new  
open-access journal

- Article-level metrics now available
- Join the conversation! Rate & comment on articles

## Thin layer thickness measurements by zero group velocity Lamb mode resonances

Maximin Cès, Dominique Clorennec, Daniel Royer, and Claire Prada<sup>a)</sup>

*Institut Langevin – Ondes et Images, Univ Paris Diderot, UMR CNRS 7587, ESPCI, 10 rue Vauquelin, 75231 Paris Cedex 05, France*

(Received 23 September 2011; accepted 19 October 2011; published online 14 November 2011)

Local and non-contact measurements of the thickness of thin layers deposited on a thick plate have been performed by using zero group velocity (ZGV) Lamb modes. It was shown that the shift of the resonance frequency is proportional to the mass loading through a factor which depends on the mechanical properties of the layer and of the substrate. In the experiments, ZGV Lamb modes were generated by a Nd:YAG pulsed laser and the displacement normal to the plate surface was measured by an optical interferometer. Measurements performed at the same point that the generation on the non-coated face of the plate demonstrated that thin gold layers of a few hundred nanometers were detected through a 1.5-mm thick Duralumin plate. The shift of the resonance frequency (1.9 MHz) of the fundamental ZGV mode is proportional to the layer thickness: typically 10 kHz per  $\mu\text{m}$ . Taking into account the influence of the temperature, a 240-nm gold layer was measured with a  $\pm 4\%$  uncertainty. This thickness has been verified on the coated face with an optical profiling system.

© 2011 American Institute of Physics. [doi:10.1063/1.3660182]

### I. INTRODUCTION

Coatings are commonly used in industrial processes for protecting surfaces against aggressive environment such as corroding media, high temperatures, friction forces, or simply wear. Over past decades, various ultrasonic techniques have been developed to characterize the deposited material. Measurements can be performed with bulk acoustic waves (BAW) and surface acoustic waves such as in acoustic microscopy<sup>1</sup> or picosecond acoustics.<sup>2,3</sup> A disadvantage of the first technique is the need for a mechanical contact with the part under test, whereas a non-contact measurement is preferable. Precise measurements on nanometric layers require high frequencies, in the GHz range, which limits the penetration depth. Thus, in acoustic microscopy and picosecond acoustics, the measurement is generally performed on the coated side of the sample.<sup>4,5</sup>

Thickness gauging of thin layers deposited on a plate can be achieved at lower frequencies (in the MHz range) by using acoustic waves guided by the structure. Non-contact generation and detection of these elastic waves with laser based ultrasonic (LBU) techniques are often used. The setup is then composed of a nanosecond pulsed laser source and an optical interferometer.<sup>6</sup> Both Rayleigh waves, guided by the coated surface, and Lamb waves, propagating along the plate-like structure, are efficient.<sup>7,8</sup> The variations of Rayleigh wave velocity or the sensitivity of Lamb mode dispersion curves are employed to measure the layer thickness and/or the elastic properties.<sup>9</sup>

It is known that resonant methods are very accurate. The most popular one is the Quartz Crystal Monitoring (QCM). The thickness of a vacuum deposited film can be determined by measuring the frequency decrease of a quartz crystal

oscillator,

$$\frac{\Delta m}{m} = \frac{\Delta \tau}{\tau} = -\frac{\Delta f}{f}, \quad (1)$$

where  $m$  is the mass per unit area of quartz crystal and  $\tau = 1/f$  its oscillation period.  $\Delta m$  is the mass per unit area of the deposited layer. This basic relation, valid while  $\Delta m/m$  is less than a few percent, indicates that the frequency decrease is independent of all mechanical properties of the deposited material except its mass. It was the original justification of the use of quartz crystals as mass-sensing devices.<sup>10</sup> The main drawback of the QCM is that the measurement can be performed only during the deposition process and not directly on the plate.

Recently, wideband electromagnetic acoustic transducers (EMATs) have been used for measuring the thickness (11  $\mu\text{m}$ ) of a polymer coating on a relatively thin (220  $\mu\text{m}$ ) aluminum sheet.<sup>11</sup> In this non-contact resonant technique, the substrate must be electrically conductive and the spatial resolution is limited by the lateral dimensions ( $>1$  cm) of the EMAT. In both QCM and EMAT techniques, the thickness resonance involved is caused by multiple reflections of longitudinal and transverse BAW between the top and bottom faces of the plate.

In this paper a LBU resonant technique using Lamb modes is proposed. It has been shown that a homogeneous isotropic plate could support Lamb modes having a zero group velocity (ZGV) for non-zero wave numbers.<sup>12</sup> Such non-propagating modes give rise to sharp local resonances that can be efficiently generated with a pulsed laser source.<sup>13</sup> For homogeneous isotropic plates, it has been demonstrated that this technique provided local measurements of material parameters and plate thickness.<sup>14</sup> A good accuracy can be achieved, since the measurement is reduced to a simple

<sup>a)</sup>Electronic mail: [claire.prada-julia@espci.fr](mailto:claire.prada-julia@espci.fr).

frequency gauging of the sample resonances in the ultrasonic domain.

The aim of this study is to apply this method to inhomogeneous samples such as a plate covered with a thin layer and to determine the film mechanical characteristics. The case studied here is composed of a thin gold layer (thickness  $<1 \mu\text{m}$ ) deposited on an isotropic Duralumin plate (thickness  $\approx 1.5 \text{ mm}$ ). This article is organized as the following: the main properties of the ZGV Lamb mode are briefly exposed in Sec. II. The variations of ZGV resonance frequency versus the layer thickness are investigated in Sec. III. The experimental setup is presented and the results are discussed in Sec. IV.

## II. ZERO GROUP VELOCITY LAMB MODES

The propagation of Lamb waves (frequency  $f$ , wavelength  $\lambda$ ) is represented by a set of dispersion curves in the angular frequency ( $\omega = 2\pi f$ ) and wave number ( $k = 2\pi/\lambda$ ) plane.<sup>15</sup> In a free homogeneous elastic plate, symmetric ( $S_n$ ) and antisymmetric ( $A_n$ ) modes satisfy two characteristic equations, first derived by Rayleigh.<sup>16</sup> It is judicious to use variables normalized to the plate thickness  $d$ , such as the frequency-thickness product  $fd = \omega d/2\pi$  and the thickness to wavelength ratio  $d/\lambda = kd/2\pi$ . Figure 1 shows the dispersion curve of the lower order modes for a Duralumin plate having longitudinal and transverse bulk wave velocities  $V_L = 6398 \text{ m/s}$  and  $V_T = 3122 \text{ m/s}$ , respectively. The  $A_0$  and  $S_0$  modes exhibit free propagation to zero frequency whereas higher order modes admit a cutoff frequency  $f_c$ , when the wave number  $k$  approaches to zero. Some branches of the dispersion curves  $\omega(k)$  exhibit minima for non-zero wave numbers. At the corresponding points, the group velocity  $d\omega/dk$  vanishes, whereas the phase velocity  $\omega/k$  remains finite. For example, the first-order symmetric ( $S_1$ ) mode exists for small wave numbers at frequencies below the transverse cutoff frequency  $f_c = V_T/d$ . The frequency decays from  $k = 0$  ( $f_c d = 3.122 \text{ MHz mm}$ ) down to a minimum at the point ( $k_0 d = 1.58$ ,  $f_0 d = 2.866 \text{ MHz mm}$ ). For wave numbers  $k < k_0$ , phase and

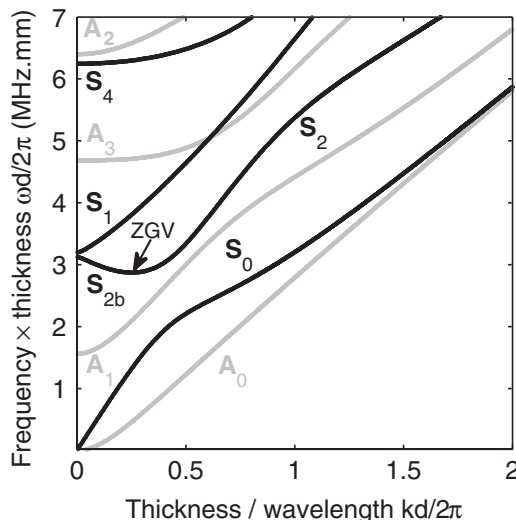


FIG. 1. Lamb mode dispersion curves for a Duralumin plate of thickness  $d$ . The arrow stands for the  $S_1 S_2$ -ZGV point.

group velocities are of opposite signs: backward propagation occurs. In the literature, the negative slope branch is classified as part of the  $S_2$  mode and is labelled  $S_{2b}$ , where  $b$  stands for “backward wave.”<sup>17</sup> At the minimum frequency of the  $S_1$ -Lamb mode, which corresponds to the junction of  $S_1$  and  $S_{2b}$  branches, a very sharp resonance can be observed. The ZGV resonance frequency is proportional to the longitudinal cut-off frequency  $f_c = V_L/2d$ , reached for  $k = 0$ . Following the American Society for Testing and Materials standard associated to the impact echo method, the multiplicative factor  $\beta$  is defined by the relation,<sup>18</sup>

$$f_0 = \beta \frac{V_L}{2d}. \quad (2)$$

In fact, other zero group velocity Lamb modes exist. The range of existence of these symmetric or antisymmetric ZGV modes and their frequency depend on the Poisson’s ratio  $\nu$ .<sup>19</sup> Clorennec *et al.* proved that the values of the resonance frequency obtained for the first two ZGV modes provided the local value of  $\nu$  and either the plate thickness  $d$  if the longitudinal and transverse velocities were known or the bulk wave velocities if the plate thickness was known.<sup>14</sup>

At the thickness resonance ( $k = 0$ ), the whole surface is vibrating in phase. Conversely, with a finite wave number, ZGV modes give rise to local resonances, having a lateral extension of about twice the plate thickness. Thus, a specific advantage of such measurements is the locality of the result.

## III. ZGV RESONANCE FREQUENCY VERSUS LAYER THICKNESS

A semi-analytical finite element method has been used to calculate the dispersion curves of Lamb waves in a bilayered structure.<sup>20</sup> The variations  $\Delta f_0$  of the ZGV resonance frequency  $f_0$  versus the layer thickness have been determined for a 1.5-mm thick Duralumin plate coated with a thin gold layer. Figure 2(a) shows, for the  $S_1 S_2$ -ZGV mode, that the relative frequency variation  $\Delta f_0/f_0$  is proportional to the mass loading,

$$\frac{\Delta f_0}{f_0} = -K \frac{\Delta m}{m}, \quad (3)$$

where  $\Delta m = \rho_2 d_2$ , with  $\rho_2$  and  $d_2$  being the mass density and the thickness of the deposited layer, respectively. This equation is similar to that stated for the quartz crystal (Eq. (1)). However, two major differences exist: the constant  $K$  is not equal to unity, even for very thin layers, and its value depends on the two materials constitutive of the bilayered structure. For the couple gold (layer) on Duralumin (substrate)  $K$  was found to be 1.16. The above linear relationship was found to be satisfactory for a relative mass load ( $\Delta m/m$ ) up to 2%, for which the deviation is about 3%. The error increases dramatically for relative mass loads larger than 10% (Fig. 2(b)).

The  $K$  factor, i.e., the proportionality factor between the relative frequency decrease and the relative mass load, was calculated for a large number of layer materials deposited on a 1.5 mm Duralumin plate. The range of variations, in between 0.3 and 1.2, indicates a large dependence of the  $K$  factor versus the mechanical parameters of the layer. Figure 3 shows that for most layer materials and within small fluctuations due

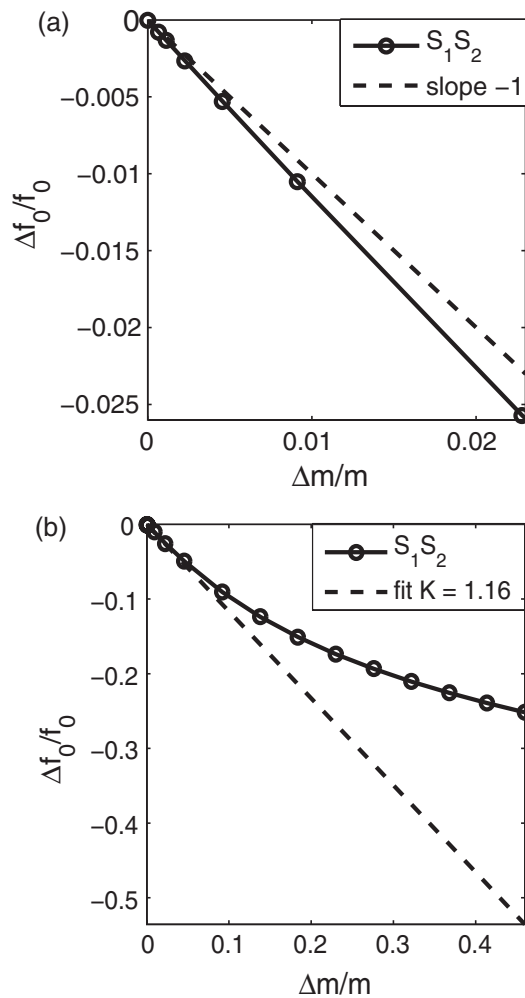


FIG. 2. Gold layer on a Duralumin plate. ZGV resonance frequency variations  $\Delta f_0/f_0$  calculated for relative mass loadings up to 2% (a), up to 45% (b).

to numerical errors, the  $K$  factor is constant in the range of mass per unit area explored:  $\Delta m = \rho_2 d_2 < 10 \text{ g/m}^2$ . The corresponding thickness is  $0.5 \mu\text{m}$  for a gold layer ( $1.5 \mu\text{m}$  for a chromium layer). Provided that the substrate and layer material parameters  $d_1$ ,  $\rho_1$ ,  $\rho_2$  are known, the layer thickness  $d_2$  can then be determined from the experimental data ( $f_0$  and  $\Delta f_0$ ) by using Eq. (3) with  $m_1 = \rho_1 d_1$ ,

$$d_2 = -\frac{1}{K} \frac{\rho_1 d_1}{\rho_2} \frac{\Delta f_0}{f_0}. \quad (4)$$

$K$  factors and material parameters used for the numerical investigations are given in Table I. The deviation from the QCM behavior ( $K = 1$ ) is very important for layers made of silicon carbide ( $K = 0.27$ ) or alumina ( $K = 0.51$ ). These materials are characterized by BAW velocities much larger than that of the substrate. Such fast layers increase the ZGV resonance frequency, while the mass loading decreases both thickness and ZGV resonance frequencies. The two effects compensate them partially. For slow layers such as gold and silver, having BAW velocities smaller than that of the substrate, the two effects add themselves. Thus the resulting  $K$  factor is larger than unity. This mechanical effect does not exist for a quartz crystal as long as the layer is located within the antinode region of

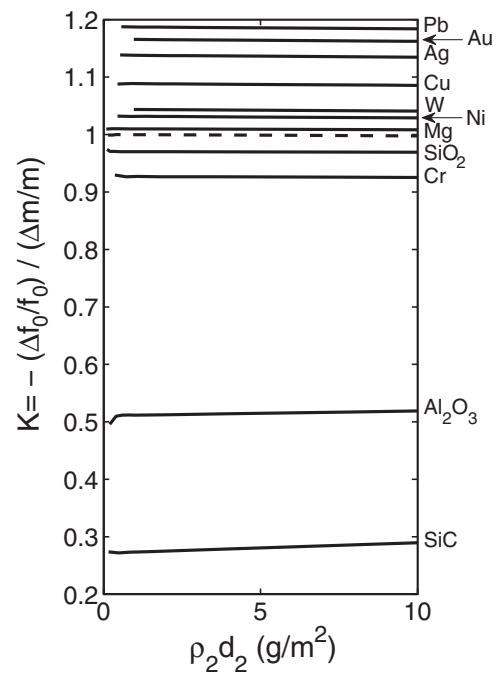


FIG. 3. Proportionality factor  $K = -(\Delta f_0/f_0)/(\Delta m/m)$  versus the mass loading ( $\rho_2 d_2$ ) for various materials deposited on a Duralumin plate of thickness  $d_1 = 1.5 \text{ mm}$ .

the mechanical displacement. As the displacement at the ZGV resonance frequency is not uniform on the plate surface,<sup>21</sup> this argument falls in the case of ZGV modes, whatever the layer thickness.

From the previous consideration, an anomalous behavior can be predicted in the case of a hard layer on a relatively soft substrate. For example, for a silicon carbide layer deposited on a copper plate, simulations performed with parameters given in Table I, lead to a negative value ( $-0.47$ ) for the  $K$  factor. In this case, the mechanical effect is larger than the mass loading and the deposit increases the ZGV resonance frequency.

For other ZGV modes ( $S_3S_6$  and  $S_5S_{10}$ ), the  $K$  factor approaches unity when the mode order increases. This behavior

TABLE I. Proportionality factor  $K$  between the relative ZGV frequency decrease  $-\Delta f_0/f_0$  and the relative mass load  $\Delta m/m$ , calculated for various layer materials deposited on a Duralumin plate (material parameters from Ref. 23).

Material	$\rho_2$ ( $\text{kg m}^{-3}$ )	$V_L$ ( $\text{m s}^{-1}$ )	$V_T$ ( $\text{m s}^{-1}$ )	$K$
Silicon carbide	3210	12099	7485	0.27
Alumina	3970	10822	6163	0.51
Chromium	7194	6608	4005	0.93
Fused silica	2150	5968	3764	0.97
Duralumin	2795	6398	3122	1.00
Magnesium	1738	5823	3163	1.01
Nickel	8907	5608	2929	1.03
Tungsten	19254	5221	2887	1.04
Copper	8933	4759	2325	1.09
Silver	10500	3704	1698	1.14
Gold	19281	3240	1200	1.16
Lead	11343	2160	700	1.19



is consistent with the fact that the corresponding ZGV resonance frequencies approach the cutoff frequencies.

#### IV. EXPERIMENTAL RESULTS AND DISCUSSION

The experimental setup is shown in Fig. 4. The source is a Q-switched Nd:YAG laser (optical wavelength 1064 nm) providing a pulse having a 20 ns duration. The transient and local heating produced by the absorption of a part of the energy deposited by the laser pulse generates Rayleigh and Lamb waves propagating in the plate. In order to generate efficiently the first ZGV Lamb mode, the spot diameter of the unfocused beam is equal to 1 mm.<sup>14,21</sup> The energy of the laser pulse is limited to 4 mJ in order to avoid any ablation of the plate surface (thermoelastic regime). Lamb waves were detected by a heterodyne interferometer equipped with a 100 mW, frequency doubled Nd:YAG laser (wavelength 532 nm, power 100 mW).<sup>22</sup> This interferometer is sensitive to any phase shift along the path of the optical probe beam reflected by the moving surface. The calibration factor for mechanical displacement normal to the surface (10 nm/V) is constant over the detection bandwidth (0.5–45 MHz). Signals are recorded by a digital sampling oscilloscope linked to a computer, which permits to process the data.

Since their group velocities vanish, Lamb waves are trapped in the source area at the ZGV resonance frequencies. Thus, if the source and detection points are superimposed, only the resonant non-propagating modes are detected after a sufficiently long time.

The sample, a 150-mm square Duralumin plate of thickness 1.503 mm, was placed on a motorized stage for the scanning, and the measurements were carried out on the bare face. Figure 5(a) shows a typical normal displacement detected at the source point after a short pulse excitation of about 20 ns and Fig. 5(b) its Fourier transform. The large oscillations observed during the first 10  $\mu$ s are due to the low frequency components of the  $A_0$  mode having small group velocities. This contribution appears in the spectrum as the continuous background. The sharpest peaks correspond to ZGV modes denoted  $S_1S_2$ ,  $S_3S_6$ , and  $S_5S_{10}$ , around 1.9 MHz, 6.3 MHz, and 10.6 MHz, respectively. At frequencies lower than 1.9 MHz, the continuous spectrum of the  $A_0$  mode dominates.

In order to measure very small deposited mass, the effect of temperature needs to be taken into account. The temperature dependence was determined at two different points

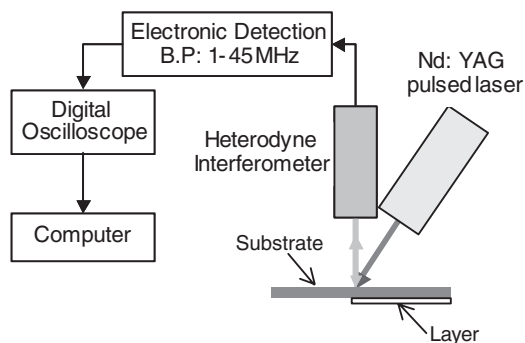


FIG. 4. Experimental setup.

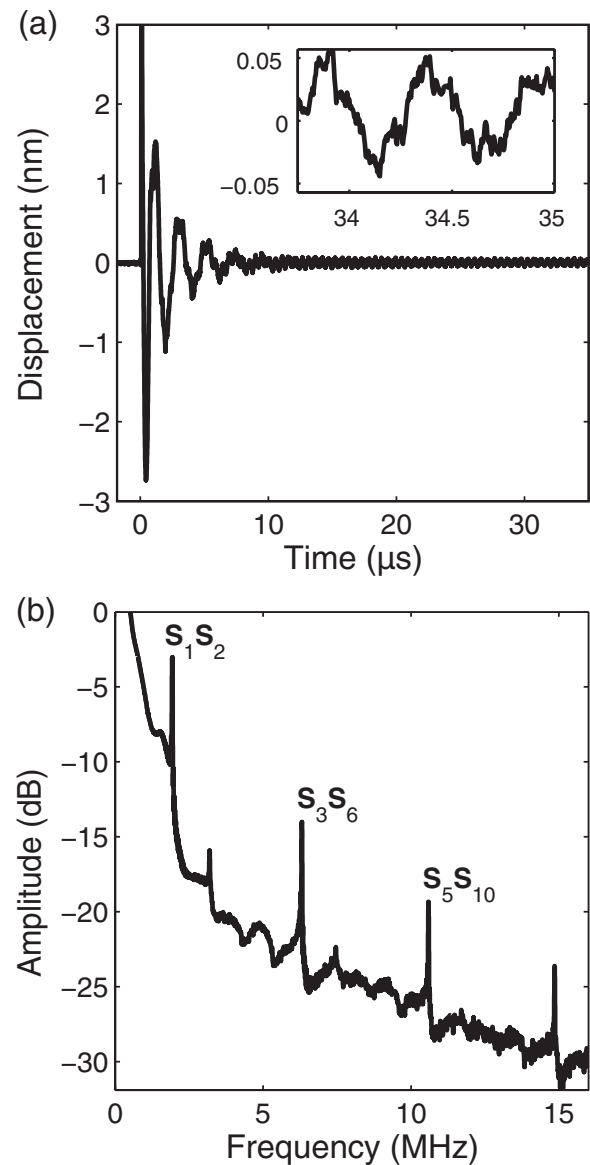


FIG. 5. Normal displacement detected at the source point on a 1.5 mm-thick Duralumin plate (a), and its Fourier transform (b).

using a thermocouple placed in thermal contact with the plate. On the first point, the temperature was varied from 19 °C to 23.5 °C while a ZGV measurement was performed. To ensure that the slope was the same for other points of the plate, the same experiment was repeated on another point and for a temperature range from 19.8 °C to 23.8 °C. The results are shown in Fig. 6. As the plate thickness was not uniform, the resonance frequencies are slightly different. The resonance frequencies vary linearly with the temperature and the slopes do not depend on the measurement point. It is now assumed that a 1° variation induces frequency shifts of 0.43 kHz for the  $S_1S_2$  resonance, 1.6 kHz for the  $S_3S_6$  resonance, and 2.5 kHz for  $S_5S_{10}$  resonance. This is consistent with the value of 0.40 kHz/K for  $S_1S_2$  deduced from the temperature dependence of Young's and shear moduli given in Balogun *et al.*<sup>21</sup> for pure aluminum. In the following experiments, the temperature variations were monitored and the corresponding frequency shifts compensated.

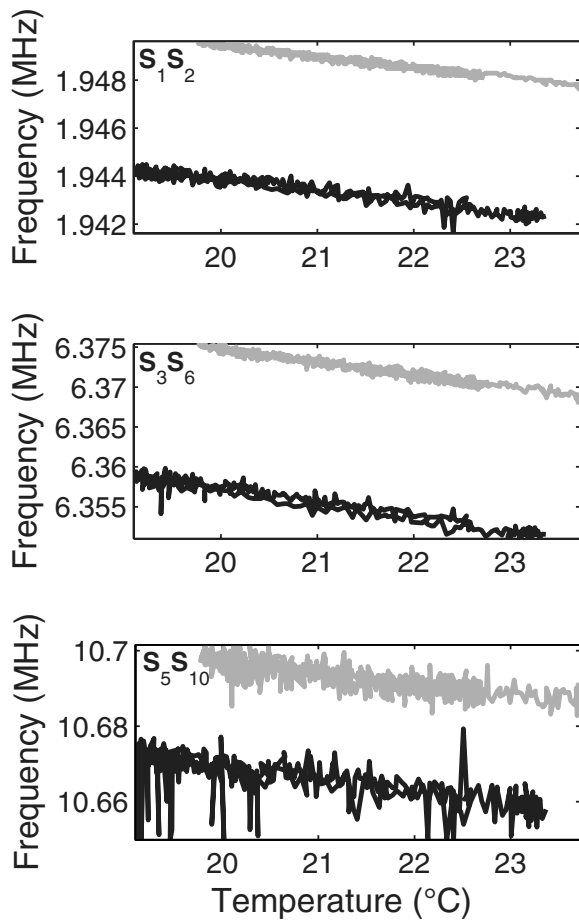


FIG. 6. Frequencies obtained for the three first ZGV modes ( $S_1S_2$ ,  $S_3S_6$ , and  $S_5S_{10}$ ) at two different positions (black and gray lines) while varying the temperature.

As the plate thickness is not uniform, a “reference scan” was acquired on one side along a 40 mm line, with 0.1 mm steps. Then a 250-nm thick gold film was deposited on the opposite side using a PVD coating machine. After the deposit, a second scan was performed on the same line. These two scans were realized so that the effect of the deposit can clearly

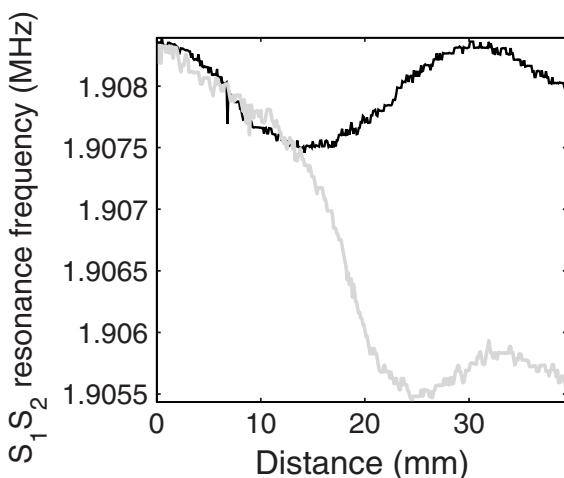


FIG. 7. Resonance frequency with respect to distance for the  $S_1S_2$ -ZGV mode, before (black line) and after (gray line) the deposit.

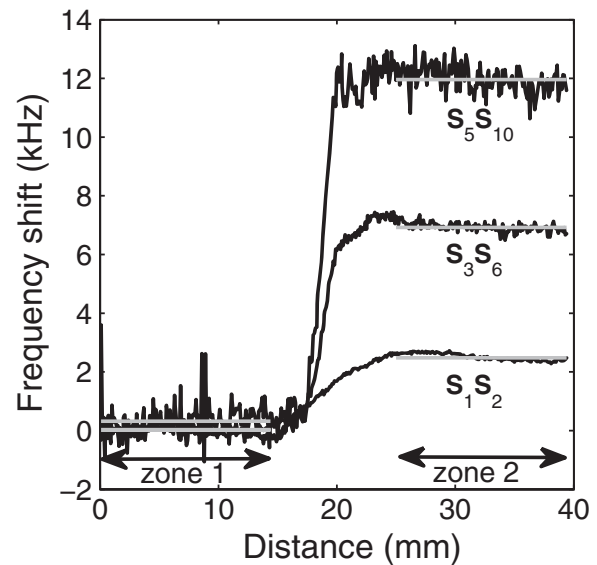


FIG. 8. Resonance frequency shifts with respect to distance for the ( $S_1S_2$ ,  $S_3S_6$ , and  $S_5S_{10}$ )-ZGV modes. Median values are indicated by gray lines.

be observed independently of the thickness variations of the plate.

The frequency scans of the sample before and after the deposit are plotted in Fig. 7 around the frequency of the first ZGV mode. A step is clearly observed since the shift is close to zero on the bare region and around a constant value for the covered region. Actually, the other ZGV modes are also affected by the deposit. The first three ZGV resonance shifts are displayed in Fig. 8. The gold-covered region can be well distinguished from the non-covered one for each ZGV resonance. The shift caused by the presence of the gold layer is about six times the one due to a 1 K-temperature variation. It was thus crucial to monitor the temperature while scanning a sample to determine correctly the thickness layer. A Wyko NT9100 Optical Profiling System has been used to verify the step profile on 0.5 mm around the border. The record, shown in Fig. 9, reveals that the step height is about 240 nm.

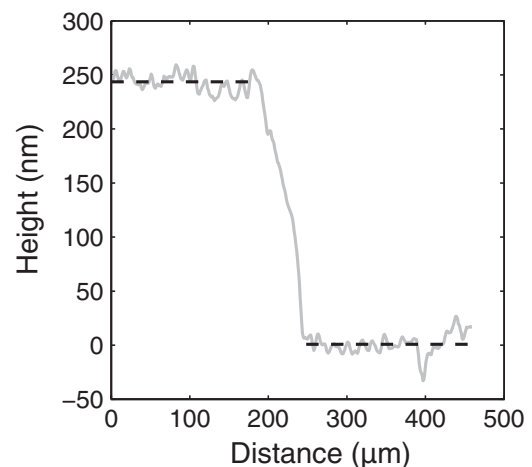


FIG. 9. Optical profile at the junction between the gold covered region and the bare one.

TABLE II. Comparison between measurements and theoretical predictions.

Mean frequency difference (kHz)	$S_1S_2$	$S_3S_6$	$S_5S_{10}$
Measured	2.46	6.88	11.65
Standard deviation	0.1	0.2	0.6
Theoretical	2.45	7.00	11.7
Relative difference (%)	0.4	1.8	0.5

In Table II, experimental results are compared to calculations for a 240-nm gold layer. The experimental values are the median of the experimental frequencies taken on zone 1 (bare) from 0 mm to 14.5 mm and on zone 2 (gold covered) from 25.0 mm to 39.5 mm. These values are plotted for each mode in Fig. 9 with dashed lines. The difference between the experimental and the predicted frequency shifts is lower than 2%, which is really good, but note that the standard deviation of the frequency found on each region is about 4% of the frequency shift for  $S_1S_2$  and  $S_5S_{10}$  mode and about 3% for the  $S_3S_6$  mode. The peaks are symmetrical and the frequency step is 50 Hz which allows a precise frequency determination, so that the error on the measurements is probably due to the surface roughness. Using formula 4 with  $K = 1.16$ ,  $f_0 = 1.908$  MHz,  $\Delta f_0 = 2.46$  kHz,  $d_1 = 1.503$  mm,  $\rho_1 = 2800$  kg m<sup>-3</sup> and  $\rho_2 = 19300$  kg m<sup>-3</sup>, we found  $d_2 = 242$  nm, which is close to the expected thickness.

## V. CONCLUSION

The effect of a thin layer on the resonance frequencies of a thick plate was investigated. Conversely to thickness resonance frequencies, the ZGV resonance frequency shift induced by the thin layer depends not only on the deposited mass but also on the substrate and the layer mechanical properties even for very thin layers. In the case of the  $S_1S_2$ -ZGV mode and up to a mass ratio of 2%, this relative frequency shift linearly depends on the relative mass ratio through a proportionality factor  $K$  which varies from 0.27 to 1.19 for a Duralumin substrate, depending on the deposited material.

Non-contact laser-based ultrasonic techniques have been used to measure the thickness of a 240 nm gold layer on a 1.5 mm thick Duralumin plate by ZGV resonance technique. The effect of temperature variations was taken into account

since, for each component of the ZGV spectrum, a one degree variation caused almost the same frequency shift as a 50-nm gold deposit. It was found that the ZGV resonance frequencies were downshifted by the deposit, allowing the estimation of the layer thickness to  $242 \pm 10$  nm. Such sensitivity with conventional ultrasound inspection by acoustic microscopy would require an operating frequency in the GHz range and measurements on the coated face. The proposed method is sensitive and can also be used on non-conductive or anisotropic substrate. Conversely to optical techniques, the experiment is executable on the bare side of the sample.

## ACKNOWLEDGMENTS

The authors would like to thank Dr. Bastien Chapuis (CEA Saclay, France) for helpful discussions.

- <sup>1</sup>Z. Yu and S. Boseck, *Rev. Mod. Phys.* **67**, 863 (1995).
- <sup>2</sup>H. T. Grahn, H. J. Maris, J. Tauc, and K. S. Hatton, *Appl. Phys. Lett.* **53**, 2281 (1988).
- <sup>3</sup>P. A. Mante, J. F. Robillard, and A. Devos, *Appl. Phys. Lett.* **93**, 071909 (2008).
- <sup>4</sup>A. Every, *Meas. Sci. Technol.* **13**, R21 (2002).
- <sup>5</sup>C. Rossignol and B. Perrin, *IEEE Trans. Ultrason. Ferroelectr. Freq. Control* **52**(8), 1354 (2005).
- <sup>6</sup>C. B. Scruby and L. E. Drain, *Laser Ultrasonics, Techniques and Applications* (Hilger, New York, 1990).
- <sup>7</sup>D. E. Chimenti, *Appl. Mech. Rev.* **50**, 247 (1997).
- <sup>8</sup>S. J. Davies, C. Edwards, G. S. Taylor, and S. B. Palmer, *J. Phys. D* **26**, 329 (1993).
- <sup>9</sup>F. Lefevre, F. Jenot, M. Ouafouh, M. Duquennoy, and M. Ourak, *Rev. Sci. Instrum.* **81**(3), 034901 (2010).
- <sup>10</sup>E. Benes, *J. Appl. Phys.* **56**, 608 (1984).
- <sup>11</sup>S. Dixon, B. Lanyon, and G. Rowlands, *Appl. Phys. Lett.* **88**, 141907 (2006).
- <sup>12</sup>S. D. Holland and D. E. Chimenti, *Ultrasonics* **42**(1–9), 957, (2004).
- <sup>13</sup>D. Clourenec, C. Prada, D. Royer, and T. W. Murray, *Appl. Phys. Lett.* **89**, 024101 (2006).
- <sup>14</sup>D. Clourenec, C. Prada, and D. Royer, *J. Appl. Phys.* **101**, 034908 (2007).
- <sup>15</sup>D. Royer and E. Dieulesaint, *Elastic Waves in Solids 1: Free and Guided Propagation* (Springer-Verlag, Berlin, 1999).
- <sup>16</sup>Lord Rayleigh, *Proc. London Math. Soc.* **20**, 225 (1889).
- <sup>17</sup>A. H. Meitzler, *J. Acoust. Soc. Am.* **38**, 835 (1965).
- <sup>18</sup>A. Gibson and J. S. Popovics, *J. Eng. Mech.* **131**(4), 438 (2005).
- <sup>19</sup>C. Prada, D. Clourenec, and D. Royer, *J. Acoust. Soc. Am.* **124**, 203 (2008).
- <sup>20</sup>G. Liu, J. Tani, T. Ohyoshi and K. Watanabe, *J. Vibr. Acoust.* **113**, 230 (1991).
- <sup>21</sup>O. Balogun, T. Murray, and C. Prada, *J. Appl. Phys.* **102**, 064914 (2007).
- <sup>22</sup>D. Royer and E. Dieulesaint, in *Proceedings of the 1986 IEEE Ultrasonics Symposium*, NY, 16–19 November 1986, p. 527, IEEE 86CH2375-4.
- <sup>23</sup>A. Briggs, *Acoustic Microscopy* (Clarendon, Oxford, 1992), p. 102.